The *kernel* root-k transformation applied to turbulent channel flows

R. S. Martins, L. Thais and G. Mompean

Laboratoire de Mécanique de Lille (LML), CNRS/FRE 3723, Université de Lille, Cité Scientifique, 59655 Villeneuve d'Ascq

Reçu le 14 novembre 2016 - Version finale acceptée le 22 février 2017

Abstract: The numerical simulation of viscoelastic fluid flows can be compromised by the loss of positive definiteness of the conformation tensor. Recent transformations to the conformation tensor have been proposed in the literature, but, to the best of our knowledge, there are no published results of turbulent drag-reducing channel flows obtained with the root-form of the general kernel transformation. We present here results for the kernel-transformed FENE-P formulation for a case with moderate elasticity at friction Reynolds number equal to 180. Although the positive definiteness of the conformation tensor was preserved, this approach diverges due to the loss of boundedness of the conformation tensor, even with the addition of an artificial diffusion term. The damping effect of the artificial diffusion ensured numerical stability, but our best results predict a significant underestimation of the relative drag reduction. Finally, the computational cost of the kernel formulation has shown to be about five times higher than the standard formulation for our algorithm.

Keywords: conformation tensor, channel flow, direct numerical simulation, kernel transformation, drag reduction, FENE-P model

[Version abrégée en Français sur la dernière page]

1. Introduction

Over the last twenty years, the Direct Numerical Simulation (DNS) of viscoelastic fluid flows has been providing relevant information on the polymer-induced drag reduction phenomenon [1, 2]. After the pioneering DNS of Sureshkumar et al. [3], several numerical works have helped to enhance the knowledge about this phenomenon: Dimitropoulos et al. [4-7], De Angelis et al. [8], Min et al. [9, 10], Dubief et al. [11], Housiadas et al. [12-15], Dallas et al. [16], Thais et al. [17-19] among others provided enriching data and discussions about the polymer-induced drag reduction. The polymer contribution to the Newtonian solvent is usually taken into account by means of a dumbbell model. Most of such models make use of a conformation tensor to describe polymer orientation [20].

By definition, the conformation tensor is Symmetric Positive Definite (SPD). Nevertheless, numerical simulations of turbulent flows of viscoelastic fluids using high-order schemes usually face non-physical high-wavenumber instabilities (the so-called Hadamard instabilities [21]) that cause the loss of the positive-definiteness of the conformation tensor. Consequently, the uncontrolled growth of the non-SPD points leads to non-physical results and the simulation usually breaks down after a few iterations.

Several proposals to overcome this issue are available in the literature. One that has been largely used is the addition of an artificial stress diffusion [22] that brings an elliptical character to the hyperbolic evolution equation of the conformation tensor. Since diffusion has no physical meaning at the simulated scales (even for a DNS), the results obtained with this method will always be confronted to the question of how intrusive this additional term is with respect to the original model [23]. A less invasive alternative is to apply the artificial diffusion only to the domain points where the SPD condition is not fulfilled (e.g. [24]). Also, alternatives without any artificial term do exist. They are usually based on flux-limiter schemes to overcome the typical exponential growth on the field of the conformation tensor due to the steep gradients inherent to high-precision simulations of viscoelastic flows [16, 25-27].

More recent solutions propose transformations to be applied to the conformation tensor in order to alleviate the steep gradients in the field of the conformation tensor, generally implying in the preservation of its positive-definiteness. This is the

case of the logarithm [28, 29], the square-root [30] and the kernel transformations [31]. Since for low Reynolds numbers there is no need (in general) to use artificial diffusion, the general kernel formulation (usually considering the root-k case) has been proven to work very well and to provide more stable simulations. It simulated successfully the Poiseuille flow in a channel, the lid-driven cavity flow and the extrudate-swell free surface flow with an Oldroyd-B fluid [32], and, more recently, the Weissenberg effect [33]. However, some of these transformations have not yet been tested in the context of turbulent viscoelastic shear flows exhibiting drag reduction, which brings us to the scope of this paper.

Housiadas et al. [15] performed simulations of polymer-induced drag-reducing channel flows using a modified version of the logarithm transformation [28, 29]. Since the square-root formulation [30] seems to be very promising [34], we test here a general version of it with the framework of the kernel formulation [31].

We evaluate here the performance of the kernel root-k formulation [31] in turbulent channel flow using a FENE-P fluid. An algorithm with spectral-like precision originally using the standard conformation tensor formulation with the addition of artificial diffusion (see [17-19]) is considered. The need for maintaining or not artificial diffusion in the kernel formulation is also assessed.

2. Mathematical modeling and numerical methods

We consider here the flow of an incompressible viscoelastic fluid in three-dimensional planar channel flow. The equations for the conservation of mass momentum are scaled with the channel half-gap, h, and the bulk velocity, U_b, and read respectively:

$$\nabla \cdot \mathbf{u} = 0 \tag{1}$$

and

$$\frac{\partial \mathbf{u}}{\partial t} + \mathbf{u} \cdot \nabla \mathbf{u} = -\nabla p + \frac{\beta}{Re_h} \Delta \mathbf{u} + \frac{1}{Re_h} \nabla \cdot \boldsymbol{\Xi} \tag{2}$$

In Eq. (2), $\beta = v_S / v_0$ is the ratio of the (Newtonian) solvent kinematic viscosity (v_S) to the total zero-shear-rate kinematic viscosity of the solution (v_0). The Reynolds number is $Re_h = hU_b / v_0$. The extra-stress tensor, $\boldsymbol{\Xi}$, represents the polymer contribution to the momentum and is accounted for by means of the Finitely Extensible Nonlinear Elastic (FENE) model with the Peterlin closure (FENE-P), yielding:

$$\boldsymbol{\Xi} = \frac{1-\beta}{Wi_h} \left[f(\mathrm{tr}(\mathbf{c}))\mathbf{c} - \mathbf{I} \right] \tag{3}$$

where $Wi_h = \lambda U_b / h$ is the bulk Weissenberg number (λ being the fluid's relaxation time), $\mathbf{c}$ is the conformation tensor representing the configuration of polymer molecules in the solution. The Peterlin function, $f(\mathrm{tr}(\mathbf{c}))$, imposes the maximum value, L, the extensibility of the molecules and reads:

$$f(\mathrm{tr}(\mathbf{c})) = \frac{L^2 - 3}{L^2 - \mathrm{tr}(\mathbf{c})} \tag{4}$$

The evolution equation for the conformation tensor assumes the form:

$$\frac{D\mathbf{c}}{Dt} + \mathbf{c} \cdot \nabla \mathbf{u} - \nabla \mathbf{u}^T \cdot \mathbf{c} + \frac{f(\mathrm{tr}(\mathbf{c}))\mathbf{c} - \mathbf{I}}{Wi_h} = 0 \tag{5}$$

The conformation tensor used to model the polymer has physical constraints that must be preserved. Because of its physical interpretation as the configuration of polymer molecules, the conformation tensor must be symmetric positive definite (SPD). However, this constraint can be violated when simulating viscoelastic fluids with moderate and high elasticity using high-order schemes. It is common to deal with the growth of non-physical high-wavenumber (Hadamard) instabilities that lead to the loss of positiveness of the conformation tensor [21].

The algorithm considered here adds an artificial diffusion term to the evolution equation of the conformation tensor. This dissipation term provides numerical stability and prevent the numerical scheme to breakdown. The evolution equation of the conformation tensor including artificial diffusion gets the form:

$$\frac{D\mathbf{c}}{Dt} + \mathbf{c} \cdot \nabla \mathbf{u} - \nabla \mathbf{u}^T \cdot \mathbf{c} + \frac{f(\mathrm{tr}(\mathbf{c}))\mathbf{c} - \mathbf{I}}{Wi_h} = \frac{D_c}{Re_h} \Delta \mathbf{c} \tag{6}$$

where $D_c = \kappa_c / v_0$ is the dimensionless stress diffusivity, κ being the dimensional diffusivity. The value of D_c is properly adjusted to preserve the positivity of the conformation tensor of at least 99% of the total number of grid points, which guarantees numerical stable simulations.

2.1 The *kernel* root-k formulation

In an effort to avoid points in which the SPD property of the conformation tensor is lost, the kernel root-k transformation proposed by Afonso et al. [31] is applied to the channel flow.

This formulation relies on the unique decomposition for the velocity gradient tensor proposed by Fattal and Kupferman [28, 29], which reads:

$$\mathbf{L} = \nabla \mathbf{u}^T = \mathbf{B} + \mathbf{\Omega} + \mathbf{N}\mathbf{c}^{-1} \tag{7}$$

where $\mathbf{L}$ is the transpose of the velocity gradient tensor, $\mathbf{B}$ is a symmetric tensor that commutes with the conformation tensor, and $\mathbf{\Omega}$ and $\mathbf{N}$ are skew-symmetric tensors. Replacing Eq. (7) into Eq. (5) yields:

$$\frac{D\mathbf{c}}{Dt} - \left(\mathbf{\Omega}\cdot\mathbf{c} - \mathbf{c}\cdot\mathbf{\Omega}\right) - 2\mathbf{B}\mathbf{c} + \frac{f(\mathrm{tr}(\mathbf{c}))\mathbf{c} - \mathbf{I}}{Wi_h} = 0 \tag{8}$$

Now, let us apply the following root transformation to the conformation tensor:

$$\mathbb{k}(\mathbf{c}) = \mathbf{c}^{\frac{1}{k}} = \mathbf{Q}_\mathbf{c}\cdot\left(\mathbf{\Lambda}^\mathbf{c}\right)^{\frac{1}{k}}\cdot\mathbf{Q}_\mathbf{c}^{\,T} \tag{9}$$

in which the operator $\mathbb{k}$ represents the kernel transformation, the tensor $\mathbf{Q}_\mathbf{c}$ is the orthogonal tensor formed by the eigenvectors of $\mathbf{c}$ in columns and that makes $\mathbf{c}$ diagonal, $\mathbf{\Lambda}^\mathbf{c}$ is the conformation tensor in its diagonal form containing its eigenvalues, and k is the degree of the root.

After some operations that are detailed by Afonso et al. [31], the evolution equation for the kernel root-k conformation gets the form:

$$\begin{aligned}&\frac{D\mathbb{k}(\mathbf{c})}{Dt} - \left(\mathbf{\Omega}\cdot\mathbb{k}(\mathbf{c}) - \mathbb{k}(\mathbf{c})\cdot\mathbf{\Omega}\right) - \frac{2}{k}\mathbf{B}\mathbb{k}(\mathbf{c})\\ &+\frac{f(\mathrm{tr}(\mathbf{c}))\mathbb{k}(\mathbf{c}) - \mathbb{k}(\mathbf{c})^{1-k}}{k\,Wi_h} = 0\end{aligned} \tag{10}$$

It is important to remark that, as pointed out by Afonso et al. [31], if one uses $k = 2$ in Eq. (10), the square-root transformation by Balci et al. [30] is recovered.

Since we are dealing with turbulent flows, for numerical stabilization purposes, an artificial stress diffusion term is added to Eq. (10), yielding:

$$\begin{aligned}&\frac{D\mathbb{k}(\mathbf{c})}{Dt} - \left(\mathbf{\Omega}\cdot\mathbb{k}(\mathbf{c}) - \mathbb{k}(\mathbf{c})\cdot\mathbf{\Omega}\right) - \frac{2}{k}\mathbf{B}\mathbb{k}(\mathbf{c})\\ &+\frac{f(\mathrm{tr}(\mathbf{c}))\mathbb{k}(\mathbf{c}) - \mathbb{k}(\mathbf{c})^{1-k}}{k\,Wi_h} = \frac{D_k}{Re_h}\Delta\mathbb{k}(\mathbf{c})\end{aligned} \tag{11}$$

where $D_k = \kappa_k/\nu_0$ is the dimensionless stress diffusivity for the kernel root-k formulation.

The set of Eqs. (1), (2) and (11) is solved by the hybrid MPI/OpenMP algorithm. The spatial discretization has spectral (Fourier) precision in the two homogenous directions (streamwise, x, and spanwise, z) and is sixth-order accurate (compact finite differences) in the wall normal, y. Time discretization is second-order accurate (Adams-Moulton scheme) to dissipative terms and also second-order accurate (Adams-Bashforth scheme) to explicit terms. The pressure is coupled to the velocity by means of a higher-order generalization of the semi-implicit fractional step method on a non-staggered grid by Armfield and Street [35]. De-aliasing and fourth-order filtering are used respectively in the non-homogenous and wall-normal directions in order to attenuate high-wave-number accumulation.

3. Results

The channel flow considered here has dimensions L_x x L_y x L_z = 8π x 2 x 3π/2 and the mesh used was N_x x N_y x N_z = 512 x 129 x 128. In the FENE-P model, the elasticity is controlled by two parameters: the maximum extensibility of the polymer molecule, L, here fixed at 30, and the zero-shear-rate friction Weissenberg number, $Wi_{\tau 0} = \lambda u_\tau^2/\nu_0$ (u_τ being the friction velocity), which was kept equal to 50. The zero-shear-rate friction Reynolds number $Re_{\tau 0} = hu_\tau/\nu_0$ was fixed at 180, corresponding to a bulk Reynolds number Re_h = 2800.

The present results are compared to the values of the public database by Thais [36]. These reference results were obtained with the original standard formulation based on the conformation tensor with the addition of artificial diffusion (following Eqs. (1), (2) and (6)). The simulations performed by Thais et al. [17-19] used the same discretization in space and time, and the artificial diffusivity necessary to maintain stability was D_c = 5.6.

We consider here three cases with the kernel formulation: two different levels of artificial diffusion with k = 2, which recovers the square root formulation [30], and one case with a fourth-order degree for the root (k = 4). A summary of the artificial diffusivity used for each case and their respective relative drag reduction is presented in Tab. 1.

Formulation	D_α	% DR
standard	5.6	28.5
kernel (k = 2)	5.6	14.0
kernel (k = 2)	2.8	17.5
kernel (k = 4)	1.4	11.6

Table 1. Relation between artificial diffusivity and relative drag reduction for cases at $Re_{\tau 0}$ = 180, L = 30, $Wi_{\tau 0}$ = 50.

In Table 1, α may be equal to $\boldsymbol{c}$ in the standard conformation tensor formulation or equal to k in the kernel root-k formulation.

It is important to note that using the same artificial diffusivity considered in the reference case with the kernel-based square-root formulation (k = 2) led to approximately half of relative drag reduction. Decreasing the artificial diffusivity by a factor of 2, the underestimation is still around 40% compared to the reference value. Moreover, when considering the degree 4 for the root, even dividing the artificial diffusivity by a factor of 4 (with respect to the value used in the standard conformation), the underestimation of the relative drag reduction is approximately 60%.

This underestimation becomes clearer when observing Figure 1, showing the profiles of the mean streamwise velocity and shear component of the Reynolds stress tensor.

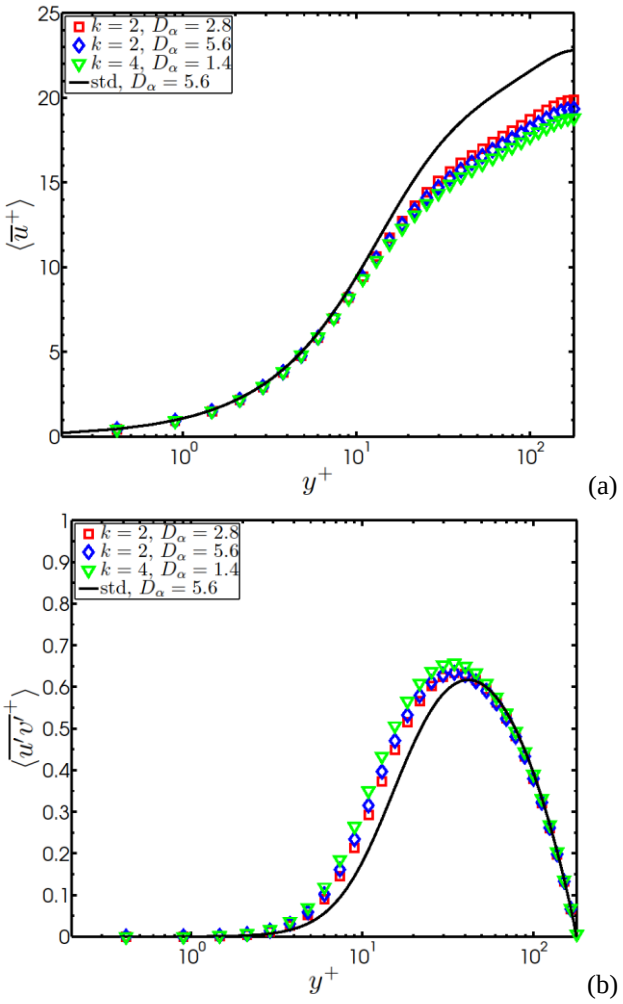

Figure 1. Profiles of the mean velocity (a) and shear component of the Reynolds stress tensor (b) in wall-units obtained with the kernel root-k (symbols) and standard (line) formulations at $Re_{\tau 0}$ = 180, L = 30, $Wi_{\tau 0}$ = 50.

Comparing to the results obtained for the velocity profile (Fig. 1a) with the standard formulation, the kernel root-k formulation provides reasonable agreement within the viscous sublayer ($0 < y^+ < 5$). However, the velocity profile is considerably underestimated in the log-law region ($y^+ < 30$).

As regards the shear component of the Reynolds stress tensor (Fig. 2a), it is noticeable that the kernel root-k formulation predicts peaks slightly closer to the wall and greater than the one calculated by the standard conformation formulation. This corroborates with the underestimation of relative drag reduction, since more energy is present in the fluctuation velocities.

The results in Table 1 and Figure 1 suggest that, for a given degree of the root, the results obtained with the kernel root-k formulation get closer to the standard formulation as the artificial diffusivity decreases. However, values of artificial diffusivity lower than the presented here for both k = 2 and k = 4 rapidly diverged due to unbounded values of the conformation tensor (limited in the FENE-P by the relation tr(**c**) < L_2). According to Vaithianathan and Collins [23], this is related to the change of sign in the restoring elastic force when the conformation tensor stretches beyond the limiting value, leading to fast numerical divergence. It is worth noting that the original algorithm with the standard conformation tensor formulation *never* presented unbounded values for the conformation tensor, which suggests that this behavior might be enhanced by the enforcement of the SPD property of the conformation tensor.

From the perspective of polymer stretch, the underestimation is also remarkable, as shown in Figure 2 containing the mean profiles of the normalized non-null components of the conformation tensor.

The normalized streamwise component of the conformation tensor (Fig. 2a) presents a value of approximately 5.5 at the wall. The standard conformation formulation predicts a peak at $y^+ \approx 10$ followed by a decrease when approaching the channel centerline. However, the results obtained with the kernel root-k formulation decrease monotonically from the wall without a peak value. Moreover, the polymer stretch in this direction is clearly underestimated with respect to the standard formulation.

For the wall-normal and spanwise stretching components (Figs. 2b and 2c, respectively), the behavior is very alike. The polymer stretch is very close to zero

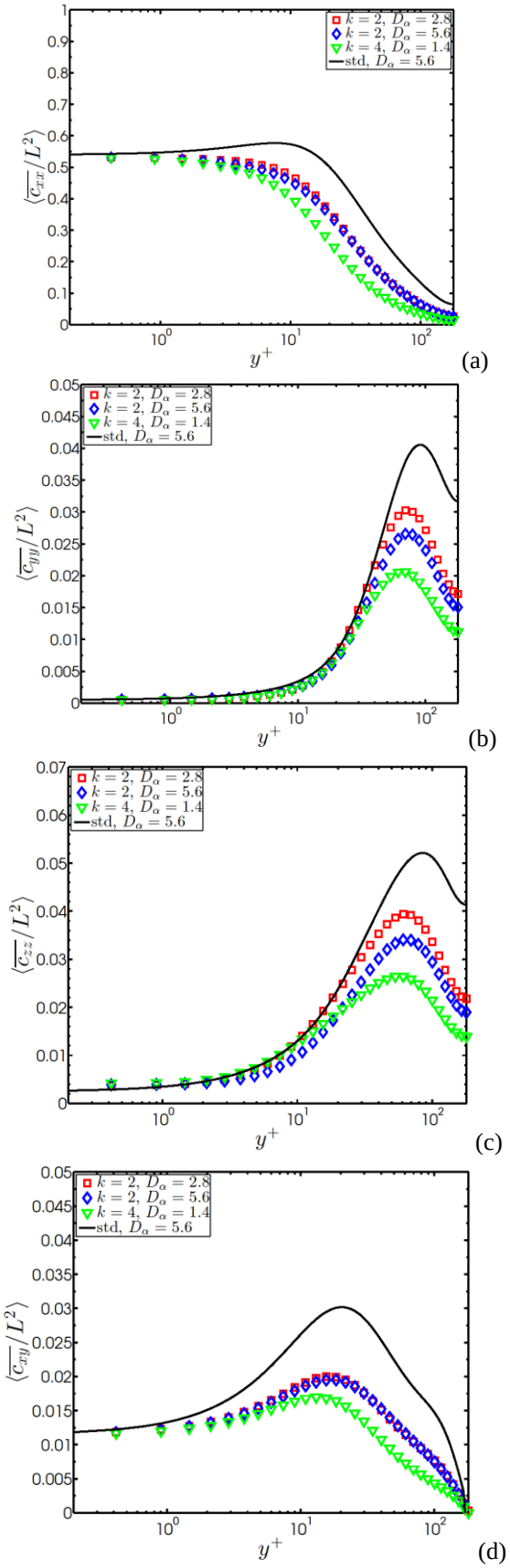

Figure 2. Profiles of the mean normalized components of the conformation tensor in wall-units obtained with the kernel root-k (symbols) and standard (line) formulations at $Re_{\tau 0} = 180$, $L = 30$, $Wi_{\tau 0} = 50$. a) streamwise, b) wall-normal, c) spanwise, d) shearwise

in these two directions. The peak value that occurs at $y^+ \approx 90$ according to the standard formulation is considerably underestimated and located closer to the wall in the kernel root-k formulation. The peak values predicted by the kernel root-k formulation are from 1/2 (for the case with $k = 4$ and $D_k = 1.4$) to 3/4 (for the case with $k = 2$ and $D_k = 2.8$) of the peak value given by the standard conformation formulation.

The shearwise component (Fig. 2d) departs from a non-zero value at the wall, increases until reaching a peak value at $y^+ \approx 20$, and decreases to zero at the channel centerline. Once again, the kernel root-k formulation underestimates the polymer stretch regardless of the artificial diffusivity.

4. Concluding remarks

We analyzed here the performance of the kernel root-k formulation applied to turbulent channel flow of FENE-P fluid. The aim of preserving the positive definiteness of the conformation tensor was achieved. With the maintenance of the SPD property of the conformation tensor, the boundedness of the conformation tensor was violated, leading to the fast divergence of the present algorithm. An artificial diffusion term was needed to maintain numerical stability, but even with this remedy, the algorithm predicts unbounded values for the conformation tensor under a certain level of diffusivity.

Since the original algorithm based on the standard conformation tensor formulation never presented unbounded values for the conformation tensor, the present results suggest that the preservation of the positive definiteness of the conformation tensor might promote the growth of unbounded values if any other special treatment is considered.

The numerically stable results achieved for root degrees of 2 and 4 presented great underestimation of the polymer stretch, velocity profile and, consequently, relative drag reduction. This underestimation can be as great as 60% of the value obtained with the standard conformation tensor formulation and is about 50% for the best case achieved in the present work.

Another worth noticing feature regards the computational cost of the tested formulation. The decomposition in Eq. (7) is usually presented on the eigenbasis of the conformation tensor [28, 29], which implies that its eigenvalues and eigenvectors must be calculated at each time step and each grid point. This operation being numerically costly, the simulations performed with the kernel root-k formulation were

about 5 times slower than the ones performed with the standard conformation tensor formulation.

A special method to guarantee the boundedness of the conformation tensor must be considered. A promising approach would be, for instance, to adapt the mapping proposed by Housiadas et al. [15] in the logarithm conformation formulation. Properly adapted and implemented, this could allow simulations with lower artificial diffusivity and, consequently, greater polymer stretch and relative drag reduction.

5. Acknowledgments

This research has granted access to the HPC resources of IDRIS under the allocation 2016-i20162b2277 made by GENCI. RSM would like to express his gratitude to João Rodrigo Andrade and Dário Canossi for their support and help with figures and equations. RSM also acknowledges the Brazilian Program "Ciência sem Fronteiras", managed by Conselho Nacional de Desenvolvimento Científico e Tecnológico (CNPq), for the financial support through grant number 200860/2012-7.

6. References

[1] Graham, M. D. Drag reduction in turbulent flow of polymer solutions. *Rheol. Reviews*, 143-170 (2004).

[2] White, C. M., Mungal, M. G. Mechanics and predictton of turbulent drag reduction whit polymer additives. *Ann. Rev. Fluid Mech.*, 40, 235-256 (2008).

[3] Sureshkumar, R., Beris, A. N., Handler, R. A. Direct numerical simulation of the turbulent channel flow of a polymer solution. *Phys. Fluids*, 9, 743-755 (1997).

[4] Dimitropoulos, C. D., Sureshkumar, R., Beris, A. N. Direct numerical simulation of viscoelastic turbulent channel flow exhibiting drag reduction: effect of the variation of rheological parameters. *J. Non-Newt. Fluid Mech.*, 79, 433-468 (1998).

[5] Dimitropoulos, C. D., Sureshkumar, R., Beris, A. N., Handler, R. A. Budgets of Reynolds stress, kinetic energy and streamwise enstrophy in viscoelastic turbulent channel flow. *Phys. Fluids*, 13, 1016-1027 (2001).

[6] Dimitropoulos, C. D., Dubief, Y., Shaqfeh, E. S. G., Moin, P., Lele, S. K. Direct numerical simulation of polymer-induced drag reduction in turbulent boundary layer flow. *Phys. Fluids*, 17, 1-4 (2005).

[7] Dimitropoulos, C. D., Dubief, Y., Shaqfeh, E. S. G., Moin, P. Direct numerical simulation of polymer-induced drag reduction in turbulent boundary layer flow of inhomogeneous polymer solutions. *J. Fluid Mech.*, 566, 153-162 (2006).

[8] De Angelis, E., Casciola, C. M., L'vov, V. S., Piva, R., Procaccia, I. Drag reduction by polymers in turbulent channel flows: Energy redistribution between invariant empirical modes. *Phys. Rev. E*, 67, 056312 (2003).

[9] Min, T., Yoo, J. Y., Choi, H., Joseph, D. D. Drag reduction by polymer additives in a turbulent channel flow. *J. Fluid Mech.*, 486, 213-238 (2003).

[10] Min, T., Yoo, J. Y., Choi. Maximum drag reduction in a turbulent channel flow by polymer additives. *J. Fluid Mech.*, 492, 91-100 (2003).

[11] Dubief, Y., White, C. M., Terrapon, V. E., Shaqfeh, E. S. G., Moin, P., Lele, S. K. On the coherent drag-reducing and turbulence-enhancing behaviour of polymers in wall flows. *J. Fluid Mech.*, 514, 271-280 (2004).

[12] Housiadas, K. D., Beris, A. N. Polymer-induced drag reduction: effects of the variations in elasticity and inertia in turbulent viscoelastic channel flow. *Phys. Fluids*, 15, 2369-2384 (2003).

[13] Housiadas, K. D., Beris, A. N. An efficient fully implicit spectral scheme for DNS of turbulent viscoelastic channel flow. *J. Non-Newt. Fluid Mech.*, 122,, 243-262 (2004).

[14] Housiadas, K. D., Beris, A. N. Characteristic scales and drag reduction evaluation in turbulent channel flow of nonconstant viscosity viscoelastic fluids. *Phys. Fluids*, 16, 1581-1586 (2004).

[15] Housiadas, K. D., Wang, L., Beris, A. N. A new method preserving the positive definiteness of a second order tensor variable in flow simulations with application to viscoelastic turbulence. *Comput. Fluids*, 39, 225-241 (2010).

[16] Dallas, V., Vassilicos, J. C., Hewitt, G. F. Strong polymer-turbulence interactions in viscoelastic turbulent channel flow. *Phys. Rev. E*, 82, 066303-1-066303-19 (2010).

[17] Thais, L., Tejada-Martinez, A., Gatski T. B., Mompean, G. A massively parallel hybrid scheme for direct numerical simulation of turbulent viscoelastic channel flow. *Comput. Fluids*, 43, 134-142 (2011).

[18] Thais, L., Gatski T. B., Mompean, G. Some dynamical features of the turbulent flow of a viscoelastic fluid for reduced drag. *J. Turb.*, 13, 1-26 (2012).

[19] Thais, L., Gatski T., Mompean, G. Analysis of polymer drag reduction mechanisms from energy budgets. *Intern. J. Heat Fluid Flow*, 43, 52-61 (2013).

[20] Bird, R. B., Hassager, O., Armstrong, R. C., Curtiss, C. F. *Dynamics of Polymeric Liquids. Kinetic theory*. 1st ed. Vol. 2, John Wiley, New York (1977).

[21] Joseph, D.D. *Fluid Dynamics of Viscoelastic Liquids*. Springer-Verlag, New York (1990).

[22] Sureshkumar, R., Beris, A. N. Effect of artificial stress diffusivity on the stability of numerical calculations and the dynamics of time-dependent viscoelastic flows. *J. Non-Newt. Fluid Mech.*, 60, 53-80 (1995).

[23] Vaithianathan, T., Collins, L. R. Numerical approach to simulating turbulent flow of a viscoelastic polymer solution. *J. Comput. Phys.*, 187, 1-21 (2003).

[24] Min, T., Yoo, J. Y., Choi, H. Effect of spatial discretization schemes on numerical solutions of viscoelastic fluid flows. *J. Non-Newt. Fluid Mech.,* 100, 27-47 (2001).

[25] Vaithianathan, T., Robert, A., Brasseur, J. G., Collins, L. R. An improved algorithm for simulating three-dimensional, viscoelastic turbulence. *J. Non-Newt. Fluid Mech.,* 140, 3-22 (2006).

[26] Yu, B., Kawaguchi, Y. Direct numerical simulation of viscoelastic drag reducing flow: a faithful finite difference method. *J Non-Newt. Fluid Mech.,* 116, 431-466 (2004).

[27] Yu, B., Li, F., Kawaguchi, Y. Numerical and experimental investigation of turbulent characteristics in a drag-reducing flow with surfactant additives. *Intern. J. Heat Fluid Flow*, 25, 961-974 (2004).

[28] Fattal, R., Kupferman, R. Constitutive laws for the matrix-logarithm of the conformation tensor. *J. Non-Newt. Fluid Mech.,* 123, 281-285 (2004).

[29] Fattal, R., Kupferman, R. Time-dependent simulation of viscoelastic flows at high Weissenberg number using the log-conformation representation. *J. Non-Newt. Fluid Mech.,* 126, 23-37 (2005).

[30] Balci, N., Thomases, B., Renardy, M., Doering, C. R. Symmetric factorization of the conformation tensor in viscoelastic fluid models. *J. Non-Newt. Fluid Mech.,* 166, 546-553 (2011).

[31] Afonso, A. M., Pinho, F. T., Alves, M. A. The *kernel*-conformation constitutive laws. *J. Non-Newt. Fluid Mech.,* 167-168, 30-37 (2012).

[32] Martins, F., Oishi, C., Afonso, A., Alves, M. A numerical study of the Kernel-conformation transformation for transient viscoelastic fluid flows. *J. Comput. Phys.,* 302, 653-673 (2015).

[33] Figueiredo, R., Oishi, C., Afonso, A., Tasso, I., Cuminato, J. A two-phase solver for complex fluids: Studies of the Weissenberg effect. *Int. J. Multiph. Flow*, 84, 98-115 (2016).

[34] Palhares Junior, I. L., Oishi, C. M., Afonso, A. M., Alves, M. A., Pinho, F. T. Numerical study of the square-root conformation tensor formulation for confined and free-surface viscoelastic fluid flows. *Adv. Model. Simul. Eng. Sci.,* 3, 1-23 (2016).

[35] Armfield, S. W., Street, R. Fractional step method for the Navier-Stokes equations on non-staggered grids. *ANZIAM J.*, 42 (E), C134-C156 (2000).

[36] Thais, L. *DNS of Newtonian and non-Newtonian turbulent channel flows up to* $Re_{\tau 0}$ = 3000. Last accessed: 27/01/15. Available on <http://lthais.plil.fr/channeldata/> (2014).

[Version abrégée en Français]

La transformation *kernel* racine-k appliquée aux écoulements turbulents en canal plan

La simulation numérique des écoulements viscoélastiques peut être compromise par la perte du caractère positif défini du tenseur de conformation. Des transformations récentes pour le tenseur de conformation ont été proposées dans la littérature, mais, à notre connaissance, il n'y a pas de résultats publiés d'écoulements turbulents en canal plan avec réduction de la traînée obtenus avec la transformation du type racine-k par la formulation générale *kernel* [Afonso et al., *J. Non-Newt. Fluid. Mech.*, (2012)]. Nous présentons ici des résultats pour le modèle FENE-P avec la transformation *kernel* pour un cas avec élasticité modérée à nombre de Reynolds de friction égal à 180. Bien que la positivité du tenseur de conformation ait été préservée, cette approche diverge en raison du caractère non-borné du tenseur de conformation, même avec l'addition d'un terme de diffusion artificielle. L'effet d'amortissement de la diffusion artificielle a permis d'assurer la stabilité numérique, mais nos meilleurs résultats prédisent une sous-estimation non négligeable de la réduction de la traînée. Enfin, le coût de calcul de la formulation *kernel* est environ cinq fois plus important que celui de l'approche standard.